PROTON TRANSPORT ACROSS CHARGED MEMBRANE AND pH OSCILLATIONS

TERESA REE CHAY, *Department of Biological Sciences, University of Pittsburgh, Pittsburgh, Pennsylvania 15260 U.S.A.*

ABSTRACT Based on Eyring's multibarrier activation process, a mathematical model and equation is developed to account for proton diffusion through an immobilized protein and enzyme membrane perfused with an electrolyte, substrate, and a buffer. With this model we find that, in the presence of a buffer, our solution approaches the continuum case very rapidly. We apply our model to membranes composed of papain and bovine serum albumin and find that our theory closely simulates the experimental observations on the effect of salt and buffer on proton diffusion. Our theory shows that the pH oscillations observed in the diffusion controlled papain-benzoyl-L-arginine ethyl ester (BAEE) reaction may be the result of CO_2 dissolved in the bath at high pH. In our theory, under certain conditions and in agreement with experimental observation, the buffer penetration depth oscillates near the boundary of a papain membrane in a solution containing BAEE and borate. We also find that at low ionic strength small ions as well as a buffer are seen to oscillate if a membrane is highly charged.

INTRODUCTION

It is generally accepted nowadays that few enzymes in vivo actually exist as free protein molecules in an aqueous environment, but they are either membrane-bound or are present in gel-like surroundings (1). Most of these bound enzymes generate, consume, or transport protons by reacting with their respective substrates. In the inner membrane of mitochondria, for example, protons are consumed by the enzymes on the M side and ejected from the energy-conserving sites on the C side of the membrane. The sites involved in the proton uptake and release face the aqueous medium which contains buffers and small ions.

Experimental and theoretical studies (2–5) reveal that the catalytic properties of bound enzymes can be quite different from those of the same enzymes in free solution. Although the free solution kinetics are not allosteric, the compartmentalized enzyme displays an apparent cooperativity in response to the variation of substrate concentration. In some cases, multiple steady states and oscillations can occur over prescribed ranges of reservoir concentration (6–10). The apparent cooperativity of a nonallosteric enzyme arises as the result of the slowness of diffusion of the species that participate in the reaction and the inhibition or activation of the enzyme by one of these species. Buffers can affect the catalytic properties of bound enzymes by acting as carriers of protons and thereby facilitating the transport of H^+ (3).

Enzymes in vivo and in vitro are frequently immobilized on charged membranes or embedded in porous media containing fixed charges, whereas many substrates and effectors in vivo and in vitro are ionized in solution. When both the support and the species are electrically charged, the concentrations of substrate and effectors in the enzymic environment can be quite different from those in the macroenvironment (i.e., in the bulk solution). Hydrophobic

and hydrophilic interactions between these species and the medium can also produce an unequal distribution of these species. This effect, which is called the partition effect, has a significant influence on the kinetic behavior of bound enzymes (11).

Our understanding of the regulation of metabolic processes in the heterogeneous cellular environment would be greatly enhanced by the analysis of transient kinetics of immobilized enzymes. Of particular biological significance are oscillations that can occur when an enzyme reaction is coupled with a membrane transport process (6). The effect of buffer and salt and their interplay on the transient catalytic activity of immobilized enzyme has not been elucidated theoretically. In this paper, we intend to study quantitatively the role of buffers and salt on the transient catalytic properties of bound enzymes. We will use Eyring's multibarrier activation process model and develop a mathematical equation which is applicable to membrane transport in general. We will then apply it to a water-permeable synthetic membrane and study the immobilized enzyme activity profile and oscillations. Our result will be compared with the experiments on the transient pH transport across synthetic membranes and the oscillations in pH observed in the papain-BAEE system (6, 7).

MATHEMATICAL DEVELOPMENT

Theoretical Model

The transport of ions across the membrane can be depicted according to the membrane transport model of Eyring and co-workers (12, 13), which views the diffusion process as a series of multiactivation steps along the Gibbs free energy profile as illustrated in Fig. 1. Here, the boundary layer is the result of the existence of unstirred water layers on the surface of the membrane. The difference in barrier heights is because of moving electrolytes which create

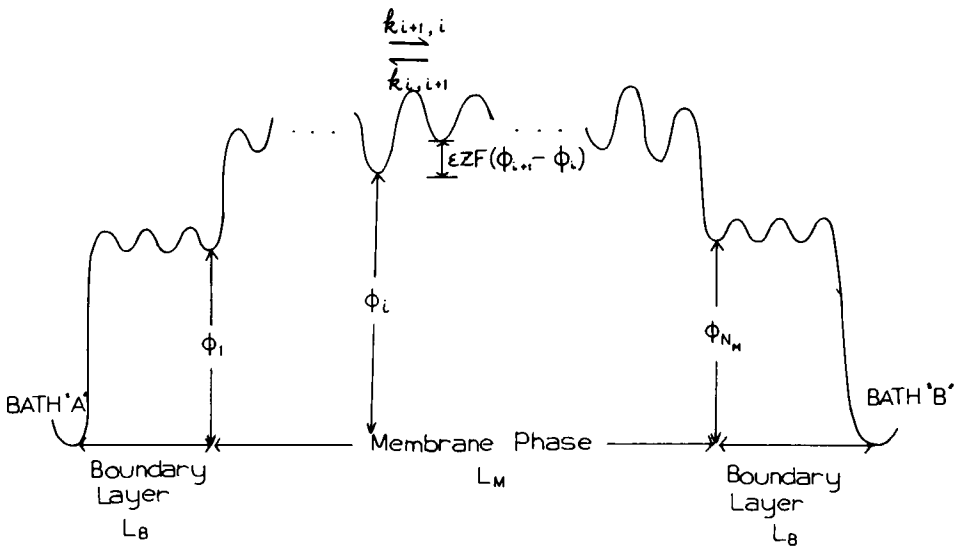

FIGURE 1 The Gibbs free-energy barriers for the diffusion process across a membrane when electrostatic fields are created by moving ions and a charged membrane. Bath A and B consist of a diffusion boundary layer, adjacent to the membrane, and a uniform bath having fixed electrolyte, buffer, and substrate concentrations.

intrinsic electric fields. The large jump between the boundary layer and the exterior of the membrane is a result of the charges on the surface of the membrane. These charges are due to the charged groups in lipids and also to the immobilized enzymes and proteins whose titratable groups and active sites face the aqueous medium. The large jump in heights between the exterior and interior of the membrane is due to a difference in dielectric constants of an aqueous and lipid phases. This barrier height difference may be estimated by the relation (14):

$$\Delta\phi_{\text{dielec}} = \frac{z^2\epsilon^2}{2b}\left(\frac{1}{D_m} - \frac{1}{D_a}\right), \tag{1}$$

where D_M and D_a are the dielectric constants for the membrane and aqueous phases, respectively, b is the ionic radius, z is the valence, and ϵ is the electronic charge.

Eq. 1 places some restrictions on the transport of ions across a membrane: In the case of a hydrophilic synthetic membrane (or the endoplasmic reticula), ions are permitted to pass through the "membrane" because $\Delta\phi_{\text{dielec}} \simeq 0$ due to the fact that $D_m \simeq D_a$. In the case of a hydrophobic membrane (such as the inner membrane of mitochondria), however, small ions are nearly impermeable to the membrane because $\Delta\phi_{\text{dielec}} \gg 0$ due to the fact that $D_m \ll D_a$. The transport of small ions across such a membrane is known to be achieved by means of channels or ionophores.

According to the model shown in Fig. 1, the change of concentration of the nth-type molecule at the ith position, $C_i^{(n)}$, with respect to time may be written as:

$$\frac{dC_i^{(n)}}{dt} = k_{i,i-1}^{(n)} C_{i-1}^{(n)} - [k_{i-1,i}^{(n)} + k_{i+1,i}^{(n)}] C_i^{(n)} + k_{i,i+1}^{(n)} C_{i+1}^{(n)} + \left(\frac{dC_i^{(n)}}{dt}\right)_{\text{reac.}} \tag{2}$$

where $(dC_i/dt)_{\text{reac}}$ is the chemical reaction such as the neutralization or enzyme-substrate reaction at the ith site, and the superscript n refers to the nth-type molecule. The term $k_{i,i-1}^{(n)}$ is the jumping rate constant from the ith site to the $i-1$st site for the nth-type molecule. (For an immobile molecule, this term is equal to zero.) In the presence of electrostatic fields, this term consists of three terms as shown below:

$$k_{i-1,i}^{(n)} = k^{(n)} \Lambda_i^{-z_n} f_{i-1}^{(n)}. \tag{3a}$$

Here, z_n is the charge that the nth-type molecule carries (it takes a plus sign if an ion carries a positive charge and a minus sign if it carries a negative charge), and Λ_i is the partition coefficient which measures the strength of electrostatic forces and takes the following expression:

$$\Lambda_i = e^{-eF(\phi_i - \phi_{i-1})/2k_BT}, \tag{3b}$$

where ϕ_i is the electrostatic potential at the ith site, F is the Faraday constant, k_BT has the usual meaning. In Eq. 3a, $k^{(n)}$ is the jumping rate constant for the nth-type molecule in the absence of electrostatic fields, and according to Eyring's absolute reaction rate theory its dependence on ionic strength is proportional to:

$$\gamma_i^{(n)}/\gamma_{i-1,i}^{(n)},$$

where $\gamma_i^{(n)}$ is the activity coefficient of the nth-type molecule at the ith site and $\gamma_{i-1,i}^{(n)}$ is that of

the activated complex formed via from the $i-1$st site to the ith site and is equal to $\gamma^{(n)}_{i,i-1}$. In usual diffusion processes, the two activities are expected to be about the same; thus, in the following development we take the ratio to be unity.

At the boundary of the two phases $k^{(n)}_{1,0}$ and $k^{(n)}_{N,N+1}$ should be multiplied by an additional factor:

$$e^{-\Delta\phi_{\text{dielec}}/RT},$$

which takes care of the difference in dielectric constants of the two media, where $\Delta\phi_{\text{dielec}}$ is given by Eq. 1. In the case of a hydrophilic membrane this factor is unity because $\Delta\phi_{\text{dielec}} = 0$.

The term $f_i^{(n)}$ in Eq. 3*a* takes care of the saturation effect for a hydrophobic membrane containing only a limited number of channels or ionophores. That is, this is a fraction of unoccupied sites and takes the following expression:

$$f_i^{(n)} = 1 - C_i^{(n)}/C^{(n)}, \tag{4}$$

where $C^{(n)}$ is the concentration of channels or ionophores which permit the nth type of ions to pass through the membrane. For a hydrophilic membrane $f_i^{(n)}$ is equal to unity.

Water-permeable Membrane Embedded with Enzymes

The following derivation is applicable to a hydrophilic synthetic membrane containing enzymes (note that the membrane which we are concerned with in this work consists of ~10% protein and ~90% water).

Let us assume that protons are generated at the ith site of the membrane in an irreversible reaction catalyzed by immobilized enzymes with the rate R_i. Further, let us assume that the protonation step is very fast compared to the diffusion and substrate-enzyme reaction steps. Then, we can combine the rate equations, Eq. 2, for all the molecules which can yield a proton. This result leads to the following equation:

$$dq_i/dt = \Delta_{i-1}(\Lambda_i) - \Delta_i(\Lambda_i^{-1}) - \Delta_i(\Lambda_{i+1}) + \Delta_{i+1}(\Lambda_{i+1}^{-1}) + R_i, \tag{5a}$$

where

$$q_i = H_i/\gamma_i^H - K_w/(\gamma_i^{OH} H_i) + B_i\bar{Z}_i^B(1) + E_i\bar{Z}_i^E + ES_i\bar{Z}_i^{ES}, \tag{5b}$$

and

$$\Delta_i(\Lambda) = k^H H_i\Lambda/\gamma_i^H - k^{OH}K_w/(\gamma_i^{OH}H_i\Lambda) + k^B B_i\bar{Z}_i^B(\Lambda). \tag{5c}$$

In deriving Eq. 5, it was assumed that all the dissociated species of buffer jump with the same jumping constant k^B. In Eqs. 5*b* and 5*c*, H_i is the activity of the hydrogen ion, B_i, E_i, and ES_i are, respectively, the concentrations of buffer, enzyme, and ES complex, γ's are the activity coefficients, K_w is the water dissociation constant, and $\bar{Z}_i^E$ and $\bar{Z}_i^{ES}$ are the charges of enzyme and ES complex at the ith site, respectively. The quantity $\bar{Z}_i^E$ takes the following expression (15):

$$Z_i^E = z_E - \bar{r}_i^E, \tag{6a}$$

where z_E is the charge of enzyme when all the titratable groups in the enzyme are occupied.

$$\bar{r}_i^E = \sum_j \frac{N_j K_j^E G_i^H}{H_i} \Big/ \left(1 + \frac{K_j^E G_i^H}{H_i}\right), \tag{6b}$$

where N_j is the number of the jth titratable group, $\bar{r}_i^E$ is the degree of dissociation of hydrogen ions per enzyme, K_j^E is the intrinsic dissociation constant of proton, and G_i^H is the correction on the dissociation constant due to the charge of the enzyme. A similar expression holds for $\bar{Z}_i^{ES}$. The term $\bar{Z}_i^B(\Lambda)$ in Eq. 5*c* is related to the net charge of buffer and takes the following expression:

$$\bar{Z}_i^B(\Lambda) = dF_i(\Lambda)/d \ln \Lambda, \tag{7a}$$

where

$$F_i(\Lambda) = \sum_{\ell=0}^{m} \Lambda^{z_B-\ell} H_i^{-\ell} \prod_{j=0}^{\ell} (K_j^B/\gamma_j) \Big/ \sum_{\ell=0}^{m} H_i^{-\ell} \prod_{j=0}^{\ell} (K_j^B/\gamma_j). \tag{7b}$$

Here, z_B is the charge of buffer when all the titratable sites are occupied, m is the total number of dissociated species, K_j^B/γ_j is the jth apparent dissociation constant ($K_0^B/\gamma_0 \equiv 1$). Note that if the system contains more than one kind of mobile buffer, the sum should be taken over the terms containing a mobile buffer (i.e., B_i term) in Eqs. 5*b* and 5*c*. Also note that if the membrane contains more than one kind of protein, the sum should be taken over the terms containing an immobile buffer (i.e., E_i term).

Because the transient behavior of H_i is of interest, we obtain the rate expression for H_i from Eq. 5*a* using a chain rule:

$$\frac{dH_i}{dt} = \Upsilon_i^{-1}\left[\Delta_{i-1}(\Lambda_i) - \Delta_i(\Lambda_i^{-1}) - \Delta_i(\Lambda_{i+1}) + \Delta_{i+1}(\Lambda_{i+1}^{-1}) - \left(\frac{dB_i}{dt}\right)\bar{Z}_i^B(1) + R_i\right], \tag{8a}$$

where

$$\Upsilon_i = 1/\gamma_i^H + K_w/\gamma_i^{OH} H_i^2 + B_i[d\bar{Z}_i^B(1)/dH_i] + E_i(d\bar{Z}_i^E/dH_i) + ES_i(d\bar{Z}_i^{ES}/dH_i). \tag{8b}$$

In Eq. 8*b*, dB_i/dt is the change of the buffer concentration with time and takes the following expression:

$$\frac{dB_i}{dt} = k^B\{B_{i-1}F_{i-1}(\Lambda_i) - B_i[F_i(\Lambda_i^{-1}) + F_i(\Lambda_{i+1})] + B_{i+1}F_{i+1}(\Lambda_{i+1}^{-1})\}. \tag{9}$$

If a buffer is consumed or produced by the enzyme reaction, R_i should be added onto the above expression. The rate equation for a substrate carrying the charge z_s may be expressed as follows:

$$d[S]_i/dt = k^s\{S_{i-1}\Lambda_i^{z_s} - (\Lambda_i^{-z_s} + \Lambda_{i+1}^{z_s})S_i + S_{i+1}\Lambda_{i+1}^{-z_s}\} - R_i, \tag{10}$$

where $[S]_i$ is the total substrate concentration (i.e., the free plus the bound substrate concentrations). Similarly, the rate equation for salt carrying z_l charges may be expressed as,

$$dI_i/dt = k^l\{I_{i-1}\Lambda_i^{z_l} - I_i[\Lambda_i^{-z_l} + \Lambda_{i+1}^{z_l}] + I_{i+1}\Lambda_{i+1}^{-z_l}\}. \tag{11}$$

In the Appendix, it will be shown that the Nernst-Planck equation comes as a first approximation to Eq. 2. We would like to point out that the model developed here is molecular and is, therefore, more general and has a higher flexibility than the Nernst-Planck equation.

Boundary Condition

Let the two sides of a membrane with thickness $2L$ face baths A and B, whose pH, substrate, buffer, and salt concentrations are fixed (see Fig. 1). This is equivalent to a model in which a membrane with thickness L is bounded on one side by an impermeable plane and on the other by a controlled pH bath. For a membrane bound to a glass pH electrode, the impermeable plane represents a glass pH electrode. Mathematically, a reflecting boundary at N+1st site means that

$$C_{N+1}^{(n)} = C_N^{(n)}, \tag{12a}$$

and

$$\phi_{N+1} = \phi_N \text{ or } \Lambda_{N+1} = 1. \tag{12b}$$

Expression for the Partition Coefficient

The rate expression for H_i in Eq. 8, B_i in Eq. 9, S_i in Eq. 10 and I_i in Eq. 11 are coupled through the partition coefficient, Λ_i. When a system is in equilibrium, the partition coefficient can be found from the Donnan equilibrium potential. When a system is in nonequilibrium, however, it can be found from the boundary condition and the electric charge neutrality condition (16, 17); i.e., the condition that the total electric charge at the ith site equals to zero:

$$\rho_i = q_i + z_s S_i + \sum z_I I_i = 0, \tag{13}$$

where the sum is taken over the positively and negatively charged salts. With Eqs. 5, 10, and 11, and with the boundary condition Eq. 12, we find the following expression from Eq. 13:

$$\Delta_{i-1}(\Lambda_i) + k^s z_s S_{i-1} \Lambda_i^{z_s} + \sum k^I z_I I_{i-1} \Lambda_i^{z_I} - \Delta_i(\Lambda_i^{-1}) - k^s z_s S_i \Lambda_i^{-z_s} - \sum k^I z_I I_i \Lambda_i^{-z_I} = 0, \tag{14}$$

from which we can find the expression for Λ_i.

APPLICATION

With the mathematical model developed in the preceding section, we intend to find the role of buffer and salt on proton transport and on pH oscillations that occur in the papain-BAEE system and compare our theoretical results with the experiments (6, 7, 18).

Enzymic Reaction

Let us consider the hydrolysis of an ester by enzyme such as chymotrypsin and papain. The reaction product is a carboxylic acid and an alcohol. The rate of the forward reaction is a function of the ester concentration as well as the hydrogen ion concentration. The rate of consumption of the substrate by these enzymes may be represented by the following

expression (19, 20):

$$\begin{array}{ccccccccc} EH_2 & & \rightleftharpoons & EH_2S & & EH_2S' & & EH_2 & \\ K_1 \downarrow\uparrow & & & \downarrow\uparrow & K_1' & \downarrow\uparrow & K_1'' & \downarrow\uparrow & \\ EH & + S & \underset{K_s(\lim)}{\rightleftharpoons} & EHS & \xrightarrow{k_2(\lim)} & EHS' & \xrightarrow{k_3(\lim)} & EH & + P_2. \\ K_2 \downarrow\uparrow & & & \downarrow\uparrow & K_2' & + & & \downarrow\uparrow & \\ E & & \rightleftharpoons & ES & & P_1 & & E & \end{array} \tag{15}$$

The apparent rate of reaction may be written as

$$R_i = k_{cat} E_T/(1 + K_{mapp}/S_i), \tag{16a}$$

where E_T is the total enzyme concentration, and

$$k_{cat} = k_2 k_3/(k_2 + k_3), \tag{16b}$$

$$k_2 = k_2\,(\lim)\,\gamma_i^{ES} \Big/ \left[\left(1 + \frac{H_i}{G_i^H K_1'} + \frac{K_2' G_i^H}{H_i}\right)\gamma_i^{ES^\ddagger}\right], \tag{16c}$$

$$k_3 = k_3\,(\lim)\,\gamma_i^{ES'} \Big/ \left[\left(1 + \frac{H_i}{G_i^H K_1''}\right)\gamma_i^{ES^\ddagger}\right], \tag{16d}$$

$$K_{mapp} = k_3 K_s G_i^s/(k_2 + k_3),$$

$$K_s = K_s\,(\lim)\left(1 + \frac{H_i}{G_i^H K_1} + \frac{G_i^H K_2}{H_i}\right) \Big/ \left(1 + \frac{H_i}{G_i^H K_1'} + \frac{G_i^H K_2'}{H_i}\right). \tag{16e}$$

Here, γ_i^{ES} and $\gamma_i^{ES^\ddagger}$ are the activity coefficients of ES complex and its activated state, respectively, and G_i^H and G_i^S are, respectively, the corrections on the dissociation constants of proton and charged substrate due to the charge of enzymes. That is, these terms take into account the fact that a net (positive) charge of enzyme will always tend to repel a positive ion and attract a negative one. An explicit expression for G_s and G_H are given by Tanford (15).

Among the parameters in the papain-BAEE reaction, $K_2' G^H$ is most sensitive to oscillations (that was previously shown by Chay [10]). Here, the quantity G^H depends strongly on ionic strength such that as the ionic strength decreases, G^H takes a value greater than unity for a positively charged enzyme, whereas it takes a value less than unity for a negatively charged enzyme. The value of the parameters for the papain-BAEE reaction was put at 25°C and 0.3 ionic strength by Whitaker and Bender (20), where $K_2' G^H$, $K_s G^s$, k_2 (lim) $\gamma^{ES}/\gamma^{ES^\ddagger}$, and k_3 (lim) $\gamma^{ES'}/\gamma^{ES^\ddagger}$ of our work corresponds to K_2', K_s (lim), k_2 (lim), and k_3 (lim) of their work. For computation of the papain-BAEE reaction, we used the value obtained by these workers with an exception of G^H, which is taken to be value greater than unity for the system at low ionic strength (i.e., for Fig. 5).

We would like to point out that our mathematical model was formulated under the assumption that the concentration of ES-complex is very low. If the concentration of ES-complex is not low, however, the rate equation for the enzyme-substrate reaction given by Eq. 16 will no longer hold. Furthermore, if the enzyme-substrate binding process occurs at about the same time as the diffusion process, the rate equation for an ES-complex should be solved along with Eqs. 8–11.

Immobilized Proteins

To compute the titration curve needed in Eq. 8, information on the intrinsic dissociation constants and on the number of titratable groups of the protein is necessary.

The following intrinsic dissociation constants were used to compute the theoretical titration curve for papain and bovine serum albumin (BSA):

α-carboxyl	3.8	sulfhydryl	9.1	
β,γ-carboxyl	4.0	ϵ-amino	9.8	
imidazolyl $\equiv NH^+$	6.9	phenolic hydroxyl	10.4	
α-amino	7.8	guanidyl $= NH_2^+$	13.0	(17)

These values came from the titration curve of BSA (21) and model compounds (22).

We expect that the number of titratable groups involved in an immobilized papain and BSA are quite different from that of the free form of these proteins for the following reasons: It is known that the immobilization with glutaraldehyde leaves a primary amino group incapable of protonation by forming an intra- and intermolecular bridge. Because glutaraldehyde has a similar reactivity as formaldehyde and the latter is known to react with an imino group (23), it is very likely that the imino groups are also incapable of protonation. Also, because of the hydrophobic nature of uncharged phenolic and ϵ-amino groups (22), many of these groups may be buried under the polymeric matrix. Furthermore, many of carboxylic and primary amino groups may not be titratable as a result of the peptide bond formation.

Because accurate information on the titration curves of immobilized papain and of BSA is not known, we have assumed that only two ϵ-amino groups of each of the proteins lose their capacity to protonate due to the immobilization. Thus, we have used the following values for the number of groups involved in the titration curve of immobilized papain (22, 24) and BSA (21):

	Papain	BSA	
α-carboxyl	1	1	
β,γ-carboxyl	13	99	
imidazolyl	2	16	
α-amino	1	1	
sulfhydryl	1	0	
ϵ-amino	7	55	
phenolic	11	19	
guanidyl	11	22	(18)

The charge and titration curve of papain and BSA were calculated by using Eq. 6 with G^H taken to be unity and using the intrinsic dissociation constants and the number of titratable groups given by Eqs. 17 and 18. The charge and the titration curve of ES complex were computed by using the intrinsic dissociation constants given by Eq. 17 with an exception of sulfhydryl group, where its dissociation constant was replaced by K_2' of Eq. 16 (because the sulfphydryl is involved in the active site of papain and K_2' corresponds to the dissociation constant of sulfhydryl group in ES complex).

Dissolved CO_2 in Solution

Carbon dioxide dissolved in an aqueous solution undergoes hydration and dissociation reactions which produce H_2CO_3, HCO_3^-, and CO_3^{2-}. At high pH, a significant amount of CO_2 in air will be dissolved in solution and will be present in an ionized form (i.e., in a form of a mobile buffer). This may affect the proton transport and play an important role in originating the pH oscillations. Since the experiments of interest for a comparison with our theory were carried out at high pH and no attempt was made to eliminate dissolved CO_2 in solution, we have considered this fact in our theoretical study.

The relation between the partial pressure of CO_2 in air and the concentration of hydrated and ionized forms of CO_2 are given by the following equations (25):

$$\begin{aligned}
[CO_2] &= P_{CO_2} Q/(1 + K_h) \\
[H_2CO_3] &= P_{CO_2} Q K_h/(1 + K_h) \\
[HCO_3^-] &= [H_2CO_3] K_1/H \\
[CO_3^{2-}] &= [HCO_3^-] K_2/H,
\end{aligned} \tag{19}$$

where K_h is the equilibrium constant for the hydration reaction, Q is Henry's constant, K_1 and K_2 are the apparent acid dissociation constants, and P_{CO_2} is the partial pressure of CO_2 in air. The values of parameters in Eq. 19 were given in the literature (25) as $K_h = 0.00258$, $Q = 10.^{-4.34}$ mm Hg^{-1}, $K_1 = 3.65$, and $K_2 = 9.97$ (at the ionic strength of ~0.1).

Eq. 19 gives only the upper limit of the actual amount of carbonate present in solution at equilibrium for the following reason. If an ideal gas were assumed, P_{CO_2} of air would be 0.251 mm Hg. At this partial pressure, we find from Eq. 19 that the concentration of dissolved CO_2 in solution at pH 9.5 and 25°C is ~0.01 M. To dissolve this much of CO_2 in a liter of solution, as much as 700 liters of fresh air should be constantly supplied and furthermore CO_2 in the air should be instantaneously hydrated at the air-solution interface. Because of the slow rate of exchange of a fresh air and of hydration reaction, however, the carbonate ions present in solution will be much less than 0.01 M and the effective P_{CO_2} which is in equilibrium with dissolved CO_2 in a bath can vary considerably. For this reason, we took P_{CO_2} to be much less than the ideal value in our computation.

The hydration reaction, i.e., $CO_2 \rightleftharpoons H_2CO_3$ is known to be much slower than the protonation reaction and is about the order of enzyme reaction (25). To simplify computation, however, we assumed it to be much faster than the enzyme-substrate reaction and the diffusion process. This assumption leads to the use of the apparent first dissociation constant $K_1^{app} = 6.21$ for H_2CO_3. (Our computation shows that this assumption is not crucial to our results.)

Numerical Methods

The differential equations developed in the preceding section were solved by a simple one-time step procedure starting from the initial concentration of buffer, salt, substrate, and hydrogen and hydroxyl ions in the bath and membrane. The initial concentration of these substances in the membrane were obtained from that in the bath by using the equilibrium condition, i.e.,

$$C_i^{(n)} = (k_{i,i-1}^{(n)}/k_{i+1,i}^{(n)}) C_{i-1}^{(n)}. \tag{20}$$

The ratio of the rate constants in Eq. 20 is related to the Donnan equilibrium potential which can be obtained from the charge neutrality condition, i.e.,

$$q_i + z_s S_i + \sum z_l I_i = 0, \tag{21}$$

by substituting Eq. 20 into Eq. 21 and with the known bath concentration of these substances. A Newton-Raphson iteration procedure was used to solve Eq. 21 for the Donnan equilibrium potential.

The initial concentration of salt in the bath were obtained by considering K^+ and Cl^- ions coming from added salt, substrate, buffer, and the pH adjustment (i.e., added KOH and HCl to bring the solution to a desired pH). The anions and cations coming from the pH adjustment were obtained as follows: Let us define the neutral pH to be that satisfying,

$$H_o + C_o = A, \tag{22a}$$

where C_o is the cation coming from the added buffer and is equal to B_o (i.e., the concentration of added buffer), and A is defined as

$$A = \frac{K_w}{H_o} + Pco_2 Q\left(\frac{K_1}{H_o} + \frac{2K_1K_2}{H_o^2}\right) - B_o(z^B - \bar{r}_o^B). \tag{22b}$$

If the pH of solution is higher than the neutral pH, the anionic concentration (coming from the adjustment) was taken to be zero and the cationic concentration was taken to be $A - H_o - C_o$. If the pH of solution is less than the neutral pH, then the cationic concentration (coming from the adjustment) was taken to be zero and the anionic concentration was taken to be $H_o + C_o - A$.

The partition coefficient Λ_i was obtained as follows: If there are only singly charged ions, Eq. 14 is very easy to solve. For a system which contains multicharged ions as well as singly charged ions, a Newton-Raphson iteration procedure was employed starting with a trial value that corresponds to a system with only singly charged ions.

The rate of jumping $k^{(n)}$ was transformed to the diffusion constant $D^{(n)}$ by using the relation

$$k^{(n)} = D^{(n)}(\Delta x)^{-2}, \tag{23a}$$

where

$$\Delta x = L/N, \tag{23b}$$

and L and N are, respectively,

$$L = L_B + L_M, \tag{23c}$$

$$N = N_B + N_M. \tag{23d}$$

Here, L_B and L_M are the thicknesses of a boundary layer and a membrane, and N_B and N_M are the number of the barriers in a boundary and membrane layers, respectively. The following values of the diffusion constants were used for computation:

$$\begin{aligned} &D^H = 5.5 \times 10^{-6}\ cm^2\ s^{-1} \\ &D^{OH} = 3.2 \times 10^{-6}\ cm^2\ s^{-1} \quad D^l = D^B = D^{OH} \\ &D^s = 1.2 \times 10^{-6}\ cm^2\ s^{-1} \end{aligned} \tag{24}$$

The values on the left column came from those measured in a diffusion cell by Naparstek et al. (6) for BSA and collodion. The diffusion constants for ionized forms of buffer and salt were assumed to be about the same as that of D^{OH}.

In Eq. 10 the total substrate concentration was taken to be equal to the free substrate concentration (i.e., $[S]_i = S_i$). This is valid because the concentration of ES complex is small all times due to a large value of K_s.

Because the terms involved in the hydrogen and hydroxyl ions (see the first two terms in Eqs. 5*b* and *c*) are negligible compared to the buffer term (i.e., the third term) and thus play only a minor role, we took $\gamma_i^H = \gamma_i^{OH} = 1$ for simplicity. We assumed that the activity coefficient of a buffer γ_j is independent of ionic strength and used the following values (25, 26) in our computation:

For carbonate:

$$K_1/\gamma_1 = 10^{-6.21} \text{ and } K_2/\gamma_2 = 10^{-9.97}$$

For borate:

$$K_1/\gamma_1 = 5.8 \times 10^{-10}$$

For phosphate:

$$K_1/\gamma_1 = 1.1 \times 10^{-2}, K_2/\gamma_2 = 1.56 \times 10^{-6}, \text{ and } K_3/\gamma_3 = 10^{-12}. \quad (25)$$

RESULTS AND DISCUSSIONS

Fig. 2 compares experimental and theoretical results on the effect of phosphate on transient proton transport across a papain-BSA immobilized membrane. The experimental values (circles) came from the data of Deem et al. (18), in which a 15-μm protein-coated pH electrode was removed at $t = 0$ from a bath at pH 6.5 and placed in a stirred bath at pH 9.5. The conditions used in our computation are identical to those used in the experiment: 15 μm membrane, 0.1 M KCl, and 25°C. The concentration of papain and BSA used are, respectively, 1 and 1.3 mM, which are consistent with the experimental values, i.e., ~10% of protein by weight and 4:1 BSA:papain ratio. To achieve a better fit to the experimental data, however, we assumed that 0.005 mm Hg CO_2 in air is in equilibrium with CO_2 dissolved in solution and that a boundary layer of thickness 15 μm exists on the surface of the membrane. The first assumption makes the curve less sigmoidal at low phosphate concentrations and the second assumption makes the curve approach equilibrium at slower rate at high phosphate concentration. (Compare this figure with Fig. 7B of reference 18, which was obtained by using Fick's law for a papain membrane in the absence of a boundary layer, carbonate buffer, and electrolytic effect.)

Note in Fig. 2 that the result is practically independent of the number of barriers in the membrane, i.e., the result using $\Delta x = 15$ μm is about the same as that using $\Delta x = 3.0$ μm. Indeed, our computation shows that the result obtained with $\Delta x = 1.5$ μm is indistinguishable from that with $\Delta x = 3.0$ μm. Note also in Fig. 2 that the presence of the phosphate buffer makes the solution approach the continuum case somewhat faster. Although it is not shown here, we found that in the absence of buffers such as carbonate or phosphate (whose pK_a lie

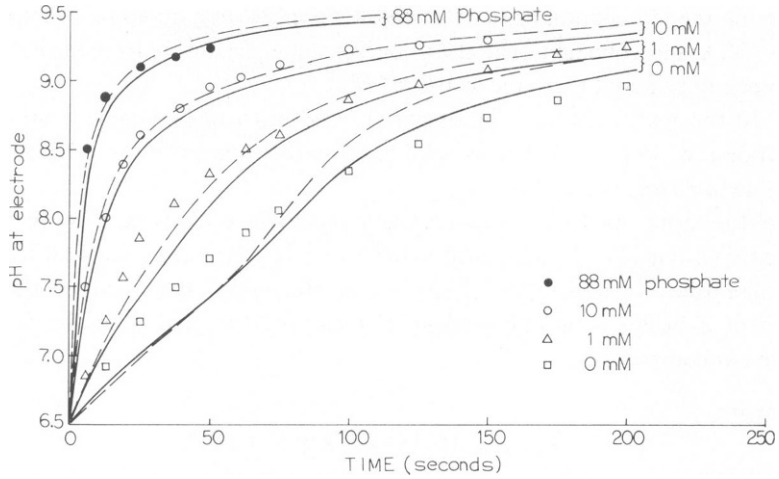

FIGURE 2 The pH at a papain–BSA-coated electrode which was initially in a bath at pH = 6.5 is placed in another bath at pH = 9.5. The experimental points came from the work of Deem et al. (18). The condition for the experiment and theory are: 0.2 M KCl, 25°C, 1 mM papain, and 1.3 mM BSA (~10% by weight BSA:papain = 4:1), the concentration of KH_2PO_4 as stated in the figure, and the thickness of membrane = 15 μm. The initial and final pH's are those shown on a papain–BSA-coated pH electrode and are not necessarily the same as pH's of the baths due to the Donnan equilibrium potential. The solid lines were computed by using $N_B = N_M = 1$, and the dashed lines were computed by using $N_B = N_M = 5$. For computation, it was assumed that $P_{CO_2} = 0.005$ mm Hg is in equilibrium with CO_2 in the bath.

between 6.5–9.5) more than several barriers are needed to obtain the continuum result. The fact that only a few barriers are needed to obtain the continuum solution makes our model applicable to the present problem. Otherwise, a huge computation time will be required to solve Eqs. 8-11 for the multibarrier case (note that there are at least 100 barriers in a membrane with a 15-μm thickness).

Fig. 3 compares the experimental and theoretical results on the effect of varying salt (KCl) concentration on how the equilibrium is approached in the absence of phosphate buffer. The experimental and theoretical conditions are identical to those of Fig. 3. Note in this figure that the experimental and theoretical relaxation times are considerably reduced at low salt concentration. Although there is a qualitative agreement on the effect of salt on proton transport, there is a considerable quantitative disagreement between the theory and experiment. That is, the dependence on ionic strength is more pronounced for the theoretical curve. This indicates that the immobilized proteins carry much less charge than was assumed in the theory. In other words, the number of titratable groups of immobilized BSA and papain is much less than that given by Eq. 18. A high charge of the membrane leads to a considerable difference in the pH's of bath and membrane at equilibrium and at low ionic strength. In the absence of added salt, for example, we found that the pH of membrane is 9.5 whereas the pH of bath is 10.22. This is due to the Donnan equilibrium potential created by a highly charged membrane at low salt concentration. At high salt concentration, however, the charge of membrane is shielded by small ions and, therefore, the two pH's at equilibrium are about the same because of reduced Donnan equilibrium potential.

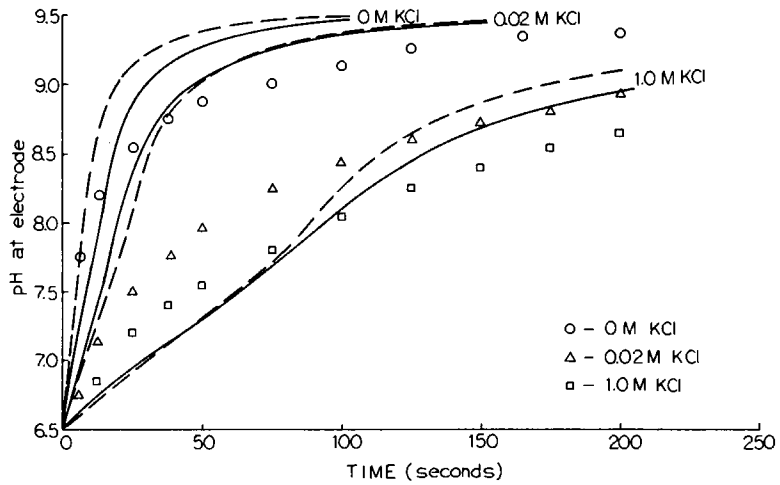

FIGURE 3 Ionic strength effect on proton transport for a papain-BSA membrane in the absence of phosphate. The experimental and theoretical conditions are the same as that of Fig. 2 and the salt concentration as stated in the figure.

Fig. 4 stimulates the pH oscillation that exists on a papain–BSA-coated electrode in the experiment by Naparstek et al. (6). The conditions used in our computation are identical to those used in the experiment: $pH_0 = 9.5$, $S_o = 4.5$ mM, KCl = 0.1 M, $L_M = 20$ μm, $E_T = 1.1$ mM (or ~10% of protein by weight), and room temperature. We find from this figure that the period and amplitude of oscillations are compatible with those of the experiment. To produce

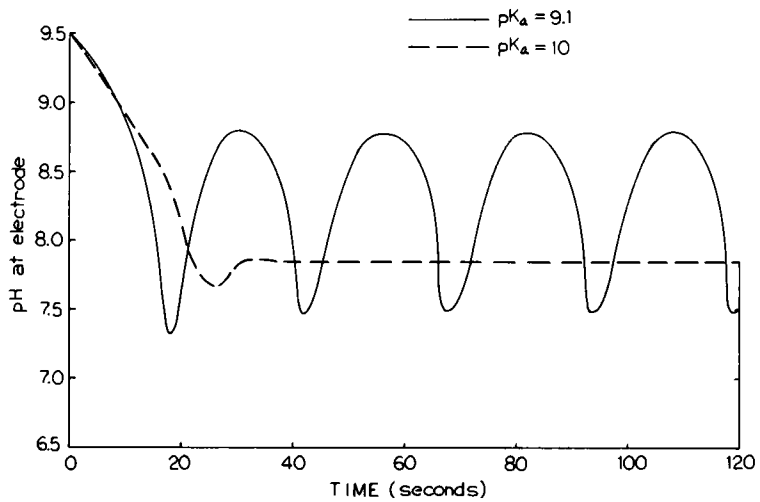

FIGURE 4 Simulation of pH oscillations on a papain–BSA-coated electrode. The conditions used for computations are the same as those of the experiment by Naparstek et al. (6): 4.5 mM BAEE, 0.1 M KCl, the length of membrane = 20 μm, $pH_0 = 9.5$, room temperature, and 1.1 mM papain. For computation, N_B and N_M were, respectively taken to be 1 and 3, and $P_{CO_2} = 0.04$ mm Hg was assumed to be in equilibrium with CO_2 in the bath.

oscillations, however, 0.04 mm Hg of P_{CO_2} was assumed to be in equilibrium with CO_2 dissolved in the bath. Without this assumption, a larger value of D^{OH} is required to produce oscillations (as previously shown by Chay [10]). This value (0.04 mm Hg) is within the limit of the partial pressure (i.e., 0.251 mm Hg of CO_2) which may be in equilibrium with CO_2 in a solution at pH 9.5 and 25°C. Note also that the theoretical curve of Fig. 4 was obtained by placing a boundary layer of length 6.67 μm. This is done to obtain a consistent result for the enzyme concentrations; i.e., in the absence of a boundary layer, much larger enzyme concentration than that used in the experiment was required to produce oscillations.

To produce oscillations, we also assumed that the imidazolyl, ϵ-amino, and phenolic groups are either reacted or buried under the matrix and hence are not capable of protonation, that the membrane is nearly electrically neutral (20 β,γ-carboxylic, 1 sulfhydryl, and 20 guanidyl), and that the pK_a of sulfhydryl (pK_a = 11) is much greater than that of model compounds (pK_a = 9.1). As shown in this figure, if the pK_a of sulfhydryl is the same as that of model compounds, oscillations do not occur. Since the sulfhydryl group of papain has a charged carboxylic group as a neighbor, it is not surprising that its pK_a is much greater than that of model compounds. This finding (that most of titratable groups need to be blocked to produce oscillations) is consistent with the conclusion drawn from Fig. 3 that the actual number of titratable groups in BSA and papain is much less than the expected value given by Eq. 18.

Fig. 5 shows oscillations in the buffer penetration depth, which occur in a polyacrylamide gel containing covalently bound papain (7, 27). The buffer penetration depth is defined by Graves et al. (7, 27) as the distance between the edge of the gel and the base band whose pH is >8.0. These workers have observed that a base band, varying in thickness, appeared along the outer perimeter of the gel, where the depths of these bands varied according to substrate and

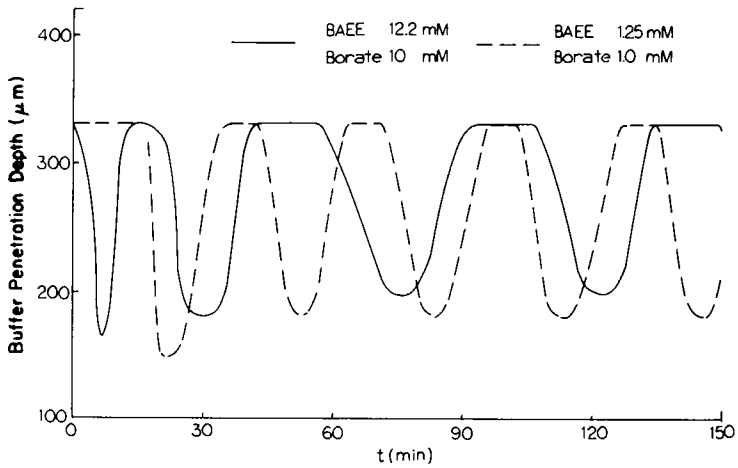

FIGURE 5 Simulation of oscillations in the buffer penetration depth. The conditions used for computation are the same as those of the experiments by Graves et al.: pH_o = 9, T = 25°C, and the borate concentrations as shown in the figure. For computation, the papain concentrations were taken to be 10 μM, N_B = 0, and N_M = 20. The substrate concentration used for computation is within the limit of that required to generate oscillations in the experiment. P_{CO_2} = 0.005 mm Hg was assumed to be in equilibrium with CO_2 in the bath.

buffer concentrations. In certain cases (i.e., 2.5 mM sodium borate and 2.5 mM BAEE; 5 mM sodium borate and 5 mM BAEE), a base band was seen to oscillate back and forth at various depths. A laser beam located at a fixed distance from the edge of the gel shows that, for a given buffer concentration, oscillations in pH seem to occur in a limited range of similar substrate concentrations.

Our theory shows that the higher a given buffer concentration is the more substrate is required to generate oscillations, in agreement with the experiment. Although the required substrate concentration (i.e., the amount required to generate oscillations) found in the theory is within the limit of that obtained in the experiment, the range of required substrate concentrations is much wider for the experiment than for the theory. This is probably due to the presence of varying amounts of CO_2 dissolved in the solution. The presence of dissolved CO_2 also plays a role in determining the range of required substrate concentrations, as can be seen from Eq. B4 of Appendix B (here $j = 1$ for borate and $j = 2$ for carbonate). In our computation, instead of varying the amount of CO_2 in the bath we assumed that a fixed concentration of carbonate is present in solution and is in equilibrium with 0.005 mm Hg of P_{CO_2} in air.

We note that to produce oscillations, a higher value of $K_2'G^H$ was used, i.e., we took G^H to be $10^{0.49}$ instead of unity. This correction is reasonable and can be explained if we take into account the fact that the two experimental conditions are not the same: The data on the papain-BAEE reaction came from the work of Whitaker and Bender (20) at high ionic strength of 0.3, whereas the oscillation experiment of Graves et al. (7) was performed in the absence of added salt. Papain enzyme is positively charged at low ionic strength, whereas its charge is shielded by small ions at high ionic strength. For a positively charged enzyme, G^H at low ionic strength should be greater than at high ionic strength, since it is a measure of ease of dissociation of a proton from an enzyme and it is easier for a proton to dissociate from a positively charged enzyme.

To save computation time the electrolytic effect was neglected, as at low enzyme concentration (10 μM concentration) Λ_i is near unity and our computation with small N_M showed that the two results (i.e., those obtained with no added salt and with an infinite amount of salt where $\lambda_i = 1$) are about the same. Furthermore, in our computation we assumed that no boundary layer exists on the surface of the membrane. This assumption is valid since unlike the experiments of Deem et al. (Figs. 2 and 3) and of Naparstek et al. (Fig. 4) where a pH electrode was immersed in a bath, a solution containing BAEE and borate at pH 9 was continuously exchanged with a fresh solution by means of a flow-through system, and therefore, no diffusion boundary exists on the surface of the membrane.

Fig. 6 shows the ion movement in a thin membrane containing only one layer enzyme (i.e., $N_M = 1$) with the concentration 1 mM. The enzyme is assumed to contain 20 β,γ-carboxylic groups, 1 sulfhydryl group and 10 guanidyl groups, and its reaction with substrate follows a Michaelis-Menten type kinetics with the following parameters:

$$K_{mapp} = K_s\left(1 + \frac{K_1'}{H} + \frac{H}{K_2'}\right)$$

$L^2k_{cat}E/D^s = 0.1$, $pK_1' = 4$, and $pK_2' = 8$. The bath contains 1 mM of substrate with one positive charge, 0.8 mM KCl, 0.1 mM phosphate at pH 10. Values of the diffusion constants

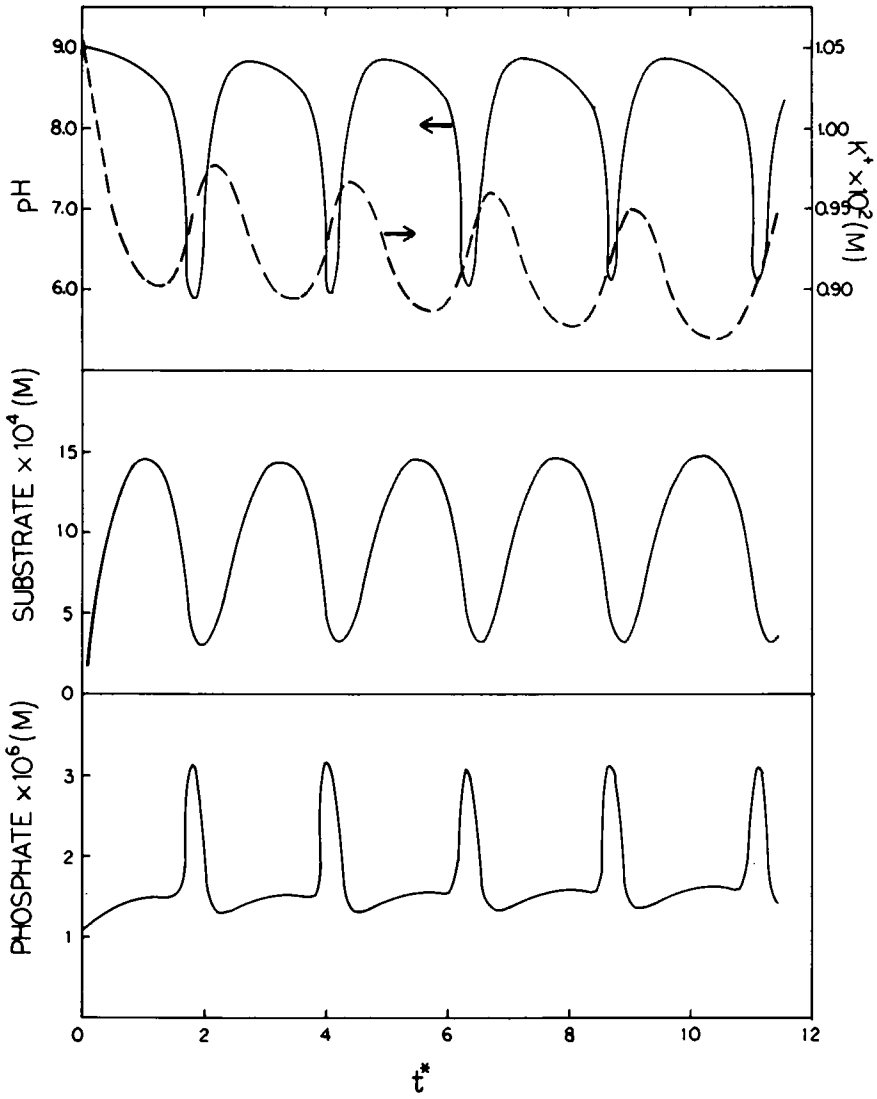

FIGURE 6 Ion movement in a membrane containing negatively charged enzymes. The bath contains 0.1 mM phosphate buffer, 0.8 mM KCl, 1 mM substrate at pH 10. The enzyme substrate reaction follows a Michaelis-Menten type kinetics with a bell-shaped pH curve. The parameters used for computation are $N_B = 0$, $N_M = 1$, $pK_1' = 4$, $pK_2' = 8$, $k_{cat} \ldots, k_{cat}L_M^2/D^S = 100$, $K_s = 0.01$ M, $E_T = 1$ mM, and $P_{CO_2} = 0$ mmHg.

used in our computation are given by Eq. 24 with an exception of D^s, which was taken to be 3.2×10^{-8} cm^{2}s^{-1}. Other parameters used for computation are $K_s = 0.01$ M and $P_{CO_2} = 0$.

In the past, oscillations similar to the ones shown in Fig. 6 have been observed in pigeon heart mitochondria in suspension (28). Our mathematical model used here corresponds to the transport of ions across a hydrophobic membrane containing a large number of channels which allow small ions as well as substrate to pass through. Thus, it is not surprising that the oscillatory phenomenon resembling that of mitochondria can be generated from our model.

Although this work is limited to proton transport across a synthetic membrane, a future application of our model should lie on proton transport in energy-transducing membrane (e.g., those of mitochondria and chloroplasts), which is a major importance to biologists and biophysicists. The present general consensus of membrane biologists is, in fact, that the activities of electron carriers of the ATPase complex in energy-transducing membranes are intimately linked with the transport of H^+ ions. In the cristae membrane of mitochondria, for example, the cytochrome oxidase centers which span the membrane are instrumental in mediating the flow of electrons from the C (or outer) side to the M (or inner) side where protonation of oxygen effectively occurs.

As for H^+-translocation itself, there are two current models, one being of course Mitchell's chemiosmotic theory for oxidative phosphorylation, the other being the so-called Bohr vectorial mechanism (29)-wherein proton translocation is due to allosteric linkage between the state (viz., the redox state) of prosthetic groups and protolytic equilibration in apoproteins (metalloproteins). In other words, there is allosteric coupling between ligand binding or redox transition of the metal atom and the pK's of the amino acid residues in the apoproteins.

When such coupling takes place in a membrane system involving a membrane bound electron translocator, the movement of electrons from one side to the other can be accomplished by H^+ movement through pK shifts in the amino acid residues of the apoprotein. This latter model could well prove amenable to analysis using the multibarrier formalism with which this work is concerned.

I would like to thank Professor Norman Zabusky for valuable comments during the progress of this work. I would also like to thank one of the referees who pointed out a possibility of application of our model to energy transducing systems (see the last three paragraphs above).

This work was supported by National Science Foundation grant PCM 76–81543.

Received for publication 8 February 1979 and in revised form 8 December 1979.

REFERENCES

1. SRERE, P. A., and K. MOSBACH. 1974. Metabolic compartmentation: symbiotic, organellar, mutienzymic, and microenvironmental. *Annu. Rev. Microbiol.* **28**:61–83.
2. GOLDMAN, R., O. KEDEM, I. H. SILMAN, S. CAPLAN, and E. KATCHALSKI. 1968. Papain-collodion membranes. I. Preparation and properties. *Biochemistry.* **7**:486–500.
3. ENGASSER, J. M., and HORVATH. 1975. Dynamic role of buffers in heterogeneous enzyme systems. *In* Analysis and Control of Immobilized Enzyme Systems. D. THOMES and J-P KERNEVEZ, Editors. Elsevier North-Holland Inc., New York. 187–197.
4. GOLDSTEIN, L., Y. LEVIN, and E. KATCHALSKI. 1964. A water-insoluble polyanionic derivative of trypsin. II. Effect of the polyelectrolyte carrier in the kinetic behavior of the bound trypsin. *Biochemistry.* **3**:1913–1919.
5. GOLDSTEIN, L., and E. KATCHALSKI. 1968. Use of water-insoluble enzyme derivatives in biochemical analysis and separation. *Z. Analy. Chem.* **243**:375–396.
6. NAPARSTEK, A., D. THOMAS, and S. R. CAPLAN. 1973. An experimental enzyme-membrane oscillator. *Biochim. Biophys. Acta.* **323**:643–646.
7. GRAVES, D. J., N. YANG, and R. A. TIPTON. 1977. Unusual modifications of immobilized enzyme kinetics caused by diffusional resistances. Preprint, University of Pennsylvania.
8. ZABUSKY, N. J., and R. H. HARDIN. 1973. Phase transition stability, and oscillations for an autocatalytic, single, first-order reaction in a membrane. *Physiol. Rev. Lett.* **31**:812–815.
9. BUNOW, B., and C. K. COLTON. 1976. Multiple steady state in cellular assays with hydrogen ion-activation kinetics. *In* Analysis and Control of Immobilized Enzyme Systems. D. THOMAS and J-P KERNEVEZ, Editors. Elsevier North-Holland Inc., New York. 41–60.
10. CHAY, T. 1979. pH oscillations in transport process. *J. Theor. Biol.* **80**:83–99.

11. ENGASSER, J. M., and C. HORVATH. 1976. Diffusion and kinetics with immobilized inzymes. *Appl. Biochem. Bioeng.* **1**:127–220.
12. PARLIN, R. B., and H. EYRING. 1954. Ion Transport Across Membranes. H. T. CLARKE, editor. Academic Press, Inc. New York. 103–118.
13. REE, F. H., T. S. REE, T. REE, and H. EYRING. 1962. Random walk and related physical problems. *Adv. Chem. Phys.* **IV**:1–66.
14. BORN, M. 1920. Volumen und hydratationswärme der ionen. *Z. Physik.* **1**:45–48.
15. TANFORD, C. 1961. Kinetics of macromolecular reactions. *In* Physical Chemistry of Macromolecules. John Wiley & Sons, New York. 526–586.
16. MACGILLIVRAY, A. D. 1968. Nernst-Plank equations and the electroneutrality and Donnan equilibrium assumptions. *J. Chem. Phys.* **48**:2903–2907.
17. ZABUSKY, N. J., and G. S. DEEM. 1979. Intrinsic electric fields and proton diffusion in immobilized protein membranes. Effect of electrolytes and buffers. *Biophys. J.* **25**:1–15.
18. DEEM, G. S., N. J. ZABUSKY, and H. STERNLICHT. 1978. Capacitance associated with proton transport in immobilized protein membranes. *J. Membr. Sci.* **4**:61–80.
19. BENDER, M. L., G. E. CLEMENT, F. J. KÉZDY, and H. D'A. HECK. 1964. The correlation of the pH (pD) dependence and the stepwise mechanism of α-chymotrypsin-catalyzed reactions. *J. Am. Chem. Soc.* **86**:3680–3690.
20. WHITAKER, J. R., and M. L. BENDER. 1968. Kinetics of papain-catalyzed hydrolysis of α-N-benzoyl-L-arginine ethyl ester and α-N-benzoyl-L-argininamide. *J. Am. Chem. Soc.* **87**:2728–2737.
21. TANFORD, C., S. A. SWANSON, and W. S. SHORE. 1955. Hydrogen ion equilibria of bovine serum albumin. *J. Am. Chem. Soc.* **77**:6414–6421.
22. TANFORD, C. 1962. The interpretation of hydrogen ion titration curves of proteins. *Adv. Protein Chem.* **17**:69–165.
23. STEVENS, C. L., T. R. CHAY, and S. L. LOGA. 1977. Rupture of base pairing in double-stranded poly(riboadenylic acid)·poly(ribouridylic acid) by formaldehyde. *Biochemistry.* **16**:3727–3739.
24. LIGHT, A., R. FRATER, J. R. KIMMEL, and E. L. SMITH. 1964. Current status of the structure of papain: the linear sequence, active sulfhydryl group, and the disulfide bridges. *Proc. Natl. Acad. Sci. U.S.A.* **52**:1276–1283.
25. EDSALL, J. T., and J. WYMAN. 1958. Carbon dioxide and carbonic acid. *In* Biophysical Chemistry. Academic Press, Inc., New York. 550–590.
26. KOLTHOFF, I. M., and P. J. ELVING. 1959. Treatise on Analytical Chemistry. Part I. John Wiley & Sons, Wiley-Interscience Div., New York. **1**:432. (Ionic strength correction added to the dissociation constant given by them.)
27. YANG, N. 1976. A study of the transient and steady state behavior of an enzyme-membrane system. M.S. Thesis, University of Pennsylvania, Philadelphia. 1–46.
28. HESS, B., A. BOITEUX, and H. G. BUSSE. 1975. Spatiotemporal organization in chemical and cellular systems. *Adv. Chem. Phys.* **XXIX**:137–168.
29. PAPA, S. 1976. Proton translocation reactions in the respitory chains. *Biochim. Biophys. Acta.* **456**:39–84.

APPENDIX A

Nernst-Planck Equation from Microscopic Approach

We intend to show that Eq. 2 with the rate expression given by Eq. 3*a* and Λ_i given by Eq. 3*b* leads to the Nernst-Planck equation at limit.

By linearizing Eq. 3*b* and using Eq. 3*a* for the rate expression, Eq. 2 becomes

$$\frac{dC_i^{(n)}}{dt} = [k^{(n)} - \xi\phi_i + \xi\phi_{i-1}]C_{i-1}^{(n)} - [2k^{(n)} + 2\xi\phi_i - \xi\phi_{i-1} - \xi\phi_{i+1}]C_i^{(n)} + [k^{(n)} + \xi\phi_{i+1} - \xi\phi_i]C_{i+1}^{(n)}, \quad \text{(A1)}$$

where $\xi = eFz_n k^{(n)}/RT$. Changing Eq. A1 to continuum and expanding $\phi(x + \Delta x)$ and $C^{(n)}(x + \Delta x)$ to the second term of Taylor expansion, we find from Eq. A1

$$\frac{\partial C^{(n)}}{\partial t} = \left[k^{(n)} - \xi \frac{d\phi}{dx}\Delta x + \frac{1}{2}\xi \frac{d^2\phi}{dx^2}\Delta x^2\right]\left[C^{(n)} - \frac{\partial C^{(n)}}{\partial x}\Delta x + \frac{1}{2}\frac{\partial^2 C^{(n)}}{\partial x^2}\Delta x^2\right]$$

$$- \left[2k^{(n)} - \xi \frac{d^2\phi}{dx^2}\Delta x^2\right] C^{(n)} + \left[k^{(n)} + \xi \frac{d\phi}{dx}\Delta x + \frac{1}{2}\xi \frac{d^2\phi}{dx^2}\Delta x^2\right]$$

$$\cdot \left[C^{(n)} + \frac{\partial C^{(n)}}{\partial x}\Delta x + \frac{1}{2}\frac{\partial^2 C^{(n)}}{\partial x^2}\Delta x^2\right]$$

$$= (k\Delta x^2)\frac{\partial^2 C^{(n)}}{\partial x^2} + (2\xi\Delta x^2)\left(\frac{d\phi}{dx}\right)\left(\frac{\partial C^{(n)}}{\partial x}\right) + (2\xi\Delta x^2)\left(\frac{d^2\phi}{dx^2}\right) C^{(n)}. \quad \text{(A2)}$$

With the Nernst-Einstein relation, i.e.,

$$\mu_n = D^{(n)}eF/RT, \quad \text{(A3)}$$

and with the identity

$$D^{(n)} = k^{(n)}\Delta x^2 \quad \text{(A4)}$$

we find from Eq. A2, the Nernst-Planck equation:

$$\frac{\partial C^{(n)}(x, t)}{\partial t} = D^{(n)}\frac{\partial^2 C^{(n)}(x, t)}{\partial x^2} + \mu_n z_n \frac{d\phi}{dx}\frac{\partial C^{(n)}(x, t)}{\partial x} + \mu_n z_n \frac{d^2\phi}{dx^2} C^{(n)}(x, t)$$

$$= \frac{\partial}{\partial x}\left[D^{(n)}\frac{\partial C^{(n)}(x, t)}{\partial x} + \mu_n z_n \phi \frac{\partial C^{(n)}(x, t)}{\partial x}\right]. \quad \text{(A5)}$$

APPENDIX B

Steady-State Analysis

If a bath contains a substrate which can react with immobilized enzymes to yield an acid, it is possible that oscillations in pH and in substrate exist. From a steady-state analysis, we intend to seek a condition for the existence of oscillations.

Omitting the time derivative from Eqs. 5*a* and 10, adding the two equations, and using the boundary condition given by Eq. 12, we find

$$\Delta_i(\Lambda_i) - \Delta_{i+1}(\Lambda_i^{-1}) + k^s[S_i\Lambda_i - S_{i+1}\Lambda_i^{-1}] = 0, \quad \text{(B1)}$$

where we have taken $z_s = 1$.

Let a system contain a buffer which has the following property: Its jth proton dissociation constant is about the same as the hydrogen ion concentration in the bath (i.e., $pH_o \simeq pK_j$), and the value of other proton dissociation constants differs greatly from that of K_j (i.e., $pK_{j-1} \ll pK_j \ll pK_{j+1}$). To simplify the analysis, we let $k^H = k^{OH} = 0$, since the terms involved in the hydrogen and hydroxyl ions are negligibly small compared to the buffer term (i.e., the first two terms in Eq. 5*c* are small compared to the last term, as long as the buffer is present in a significant amount). Further, we let $i = 0$ in Eq. B1. Then, this leads to the following expression:

$$H_1^* = \frac{1}{d}\left\{K_j^* k^s(S_0 - S_1\Lambda_1^{-2}) - \frac{k^B B_0 K_j^*}{1 + K_j^*}\right.$$

$$\left.\cdot [jK_j^*(\Lambda_1^{-j-1} - \Lambda_1^{j-1}) + (j - 1)\Lambda_1^{-j} - j\Lambda_1^{j-1}]\right\}, \quad \text{(B2)}$$

where

$$d = -k^s(S_0 - S_1\Lambda_1^{-2}) + \frac{k^B B_0}{1 + K_j^*} \cdot \{K_j^*[j\Lambda_1^{-j-1} - (j-1)\Lambda_1^{j-2}] + (j-1)(\Lambda_1^{-j} - \Lambda_1^{j-2})\}, \quad \text{(B3)}$$

and H_1^* and K_j^* are, respectively, defined as H_1/H_0 and K_j/H_0. Note from Eq. B2 that H_1^* becomes very large as the denominator approaches zero. That is, a singularity exists in the expression of H_1^* if $d = 0$, i.e., if S_o and B_o satisfy the following relations:

$$k^s S_o = \frac{k^B B_o}{(1 + K_j^*)(1 - S_1^*\Lambda_1^{-2})} \cdot \{K_j^*[j\Lambda_1^{-j-1} - (j-1)\Lambda_1^{j-2}] + (j-1)(\Lambda_1^{-j} - \Lambda_1^{j-2})\}, \quad \text{(B4)}$$

where $j = 1$ for borate and $j = 2$ for carbonate if the pH of a bath were near 9. Eq. B4 shows that for a given buffer concentration only a limited amount of substrate can generate oscillations and that the required substrate concentration (i.e. that needed to generate oscillations) is linearly dependent on the buffer concentration at a fixed salt concentration. Note that at high ionic strength, the charge of a membrane does not influence the required substrate concentration since the electrolytic term Λ_1 is near unity. At low ionic strength, however, the required substrate concentration depends on the charge of a membrane, since $\Lambda_1 \gg 1$ if the membrane is positively charged and $\Lambda_1 \ll 1$ if it is negatively charged.